Integrated Bioinformatics Analysis for Potential Target Genes of In-Stent Restenosis

Chenxi Liu
Department of Cardiovascular Medicine, Xiangya Hospital, Central South University, Changsha, Hunan 410008, P.R. China

Yuanyuan Kuang
Department of Cardiovascular Medicine, Xiangya Hospital, Central South University, Changsha, Hunan 410008, P.R. China

Yubo Liu
Department of Cardiovascular Medicine, Xiangya Hospital, Central South University, Changsha, Hunan 410008, P.R. China

Yi Peng
From the Rheumatology and Immunology (T.X.), Xiangya Hospital, Central South University, Changsha, Hunan, China.

Yinzhuang Zhang
Department of Cardiovascular Medicine, The First Hospital of Changsha, Changsha, Hunan 410005, P.R. China.

Haodong Gao
Department of Cardiovascular Medicine, Xiangya Hospital, Central South University, Changsha, Hunan 410008, P.R. China

Xiangyu Yang
Department of Cardiovascular Medicine, Xiangya Hospital, Central South University, Changsha, Hunan 410008, P.R. China

Jia Tang
Department of Cardiovascular Medicine, Xiangya Hospital, Central South University, Changsha, Hunan 410008, P.R. China

Li Ma
Department of Cardiovascular Medicine, Xiangya Hospital, Central South University, Changsha, Hunan 410008, P.R. China

Qilin Ma (mqilin2004@163.com)
Department of Cardiovascular Medicine, Xiangya Hospital, Central South University, Changsha, Hunan 410008, P.R. China

---

Research Article

Keywords: ISR, PCI, Bioinformatics, Genomics

Posted Date: June 3rd, 2022

DOI: https://doi.org/10.21203/rs.3.rs-1664073/v1

Integrated Bioinformatics Analysis for Potential Target Genes of In-Stent Restenosis

Chenxi Liu[1,2], Yuanyuan Kuang[1], Yubo Liu[1,2], Yi Peng[2,3], Yinzhuang Zhang[4], Haodong Gao[1,2], Xiangyu Yang[1,2], Jia Tang[1,2], Li Ma[1,2], Qilin Ma[1,2*].

1. Department of Cardiovascular Medicine, Xiangya Hospital, Central South University, Changsha, Hunan 410008, P.R. China.

2. National Clinical Research Center for Geriatric Disorders, Xiangya Hospital, Changsha, Hunan, P.R. China, 410008.

3. Department of Rheumatology and Immunology (T.X.), Xiangya Hospital, Central South University, Changsha, Hunan 410008, P.R. China.

4. Department of Cardiovascular Medicine, The First Hospital of Changsha, Changsha, Hunan 410005, P.R. China.

Correspondence to: Qilin Ma. Department of Cardiovascular Medicine, Xiangya Hospital, Central South University, Changsha, Hunan 410008, P.R. China; National Clinical Research Center for Geriatric Disorders, Xiangya Hospital, Changsha, Hunan, P.R. China, 410008. Email: mqilin2004@163.com.

Abstract

Background: In-stent restenosis (ISR) is a common complication after percutaneous coronary intervention (PCI), which greatly affects the patients after PCI. Here, we extracted the left internal mammary artery (LIMA) from 4 coronary artery bypass graft (CABG) patients with stable angina and 3-vessel coronary atherosclerotic lesions, implanted bare-metal stents (BMS) or paclitaxel

drug-eluting stents (PES), and analyzed their tissue differentially expressed genes (DEGs) to explore the possible mechanism and pathway of ISR formation.

Methods: To figure out the effects of BMS and PES on vascular tissue and find the potential target genes for ISR, we explored DEGs from GSE19136 by comparing LIMA tissues implanted two stents. All DEGs were divided into up-regulating group and down-regulating group and enriched respectively in Gene Ontology (GO) terms and Kyoto Encyclopedia of Genesand Genomes (KEGG). Gene set enrichment analysis (GSEA) was aimed at all gene expression data. Constructing the PPI network of two groups of DEGs, we identified several hub genes and predicted their regulating miRNAs and key transcription factors (TFs) regulators in the online database. Additionally, we used RT-PCR to validate hub genes expression in two models of endothelial (EC) inflammation and vascular smooth muscle (VSMC) proliferation, which simulated the mechanism of ISR.

Results: The datasets had a total of 759 DEGs (log2|foldchange(FC)| > 1 and *P* value < 0.05) identified, including 389 up-regulated and 370 down-regulated DEGs, Bioinformatics analysis result shows relevant genes function and identified hub genes and their regulating factors. Finally, RT-PCR validated that there were significant differences in the expression of LIF, CENPE, KIF11, MMP3, MCM10, and ARHGAP11A in the constructed cell model of EC inflammation, while GTSE1, GINS2, RRM2 and CKAP2L in the model of VSMC proliferation (*P* value < 0.05). Conclusion: Here, using comprehensive bioinformatics analysis and functional enrichment, We found the potential target genes (LIF, CENPE, KIF11, MMP3, MCM10, ARHGAP11A, GTSE1, GINS2, RRM2 and CKAP2L) inherent ISR by comparing LIMA tissues implanted with different

stents in GSE19136. We identified several potential genes, which are worthy of new exploration for the prevention of ISR in the future.

Keywords: ISR, PCI, Bioinformatics, Genomics.

INTRODUCTION:

In-stent restenosis (ISR) is the gradual renarrowing of a stented coronary artery lesion from arterial damage with subsequent neointimal tissue proliferation[1]. The application of drug-eluting stent (DES), including paclitaxel-eluting stent (PES), sirolimus-eluting stent (EES), dramatically reduce ISR and target vessel revascularization compared with bare-metal stents (BMS)[2]. Even though, the overall rate of in-stent restenosis following stent implantation remains high[3]. Meanwhile, the rapid implementation of DES in standard practice leads to DES in-stent restenosis (ISR), which occurs in 3% to 20% of patients, depending on patient and lesion characteristics and DES type[1].

At present, it is believed that the occurrence of ISR is related to inflammation, endothelial cells (EC) dysfunction, vascular smooth muscle cells (VSMC) proliferation and migration. some studies have shown that some substances can inhibit the formation of ISR. Inhibiting VSMC phenotype modulation and proliferation by down-regulating the expression of proliferating cell nuclear antigen (PCNA) and up-regulating that of p27kip1 may reduce ISR[4]. Some immune diseases may also induce ISR[5] and drastically reducing inflammatory reactions may reduce the occurrence of ISR[6]. Suppressing in-stent neointimal growth by limiting local inflammatory pathways may be useful in patients undergoing percutaneous interventions[7]. Tumor necrosis factor-alpha (TNF-α) leads to EC dysfunction which might be a predictor of

restenosis[8-9]. At the same time, some miRNAs also play potential but essential roles in ISR and inflammation in stented arteries[2].

However, the specific mechanism of ISR is not clear, especially why different stents lead to ISR. Here, we tried to use bioinformatics to analyze array based on expression array database and screen some valuable genes. These gene expression characteristics help to find new targets for the treatment of ISR and create therapeutic strategies.

MATERIALS AND METHODS

Data source

The array expression data sets (GSE19136) were downloaded from the Gene Expression Omnibus (GEO) database. A total of 4 human left internal mammary arteries (LIMA) samples were collected from 4 different coronary artery bypass graft (CABG) patients with stable angina and 3-vessel coronary atherosclerosis. Each LIMA was divided into three segments, and two of the segments were fitted with either a PES or a BMS. The experiment includes three groups: control, PES and BMS, respectively. Each group includes four biological replicates. The data were analyzed with Expression Console ver.1 using Affymetrix default analysis settings followed by MAS5 as the normalization method. The trimmed mean target intensity of each array was arbitrarily set to 100. The three datasets were all quantile normalized and log2-transformed.

Data pre-processing

Differentially expressed gene analysis

Data pre-processing consisted of three steps: transition from gene probes to gene symbols, data consolidation, and normalization. First, the series matrix files were annotated with an official gene symbol using the data table of the array platform, and the gene expression matrix files were

obtained. Gene probes without gene symbols or genes with more than one probe were eliminated or averaged, respectively. The gene expression matrix files of three segments were normalized and Log2-transformed with R language (R i386 4.0.5).

The differentially expressed genes (DEGs) between BMS group and PES group were determined using the limma package[10] in R. The thresholds were log2 |foldchange (FC)| > 1 and *P* value < 0.05. DEG visualization was done using a volcano map and heatmap using ggplot2[11] and the pheatmap package[12].

Functional enrichment analysis of DEGs

The clusterprofiler R package[13], the stringr[14] R package and the database for annotation, visualization, and integrated discovery[15] were used to functionally enrich and analyze the enriched pathways of the key DEGs in Gene Ontology (GO) terms and Kyoto Encyclopedia of Genesand Genomes (KEGG). The threshold was *P* value < 0.05.

PPI network construction and analysis

To explore the interacting genes, the search tool STRINGS[16] was employed to establish a DEG PPI network, which was finished using Cytoscape[17]. Interaction with a combined score > 0.4 was set as the cut-off point. The most important module in the PPI network was identified using the plug-in Molecular Complex Detection (MCODE)[18] of Cytoscape, an application to cluster a given network by topology, to find densely connected regions. The criteria for selection were as follows: MCODE scores > 4, degree cut-off = 2, node score cut-off = 0.2, max depth = 100, and k-score = 2. Subsequently, the maximal clique centrality (MCC) algorithm of CytoHubba[19] was used to explore the PPI network hub genes.

Gene set enrichment analysis

Gene set enrichment analysis (GSEA)[20] was performed using GSEA 4.2.3 software. Enrichment results satisfying a nominal *P*-value cut-off of < 0.05 were considered statistically significant. MSigDB was downloaded from http://www.gsea-msigdb.org/gsea/downloads.jsp.

Regulating miRNA prediction

The online prediction tool microRNA Data Integration Portal (mirDIP) (http://ophid.utoronto.ca/mirDIP)[21] was used to predict potential microRNA (miRNA) targeting. The hub genes of up-regulation and down-regulation were submitted respectively and the top five predicted miRNAs of each hub gene were chosen and listed.

Key transcription factors (TFs) regulators prediction

The online dataset TRRUST (version 2) (https://www.grnpedia.org/trrust/)[22] was used to find potential key TF regulators of hub genes. We submit all hub genes and all regulators were be listed.

Cell culture

Human Umbilical Vein Endothelial Cells (HUVECs) were seeded on 6-well plates in F12 medium, 5% FBS, 2% penicillin and streptomycin. Rat thoracic artery smooth muscle cells line (A7r5) were cultured in 6-well plates in DMEM (4500mg/L D-glucose, 1500mg/L NaHCO3), 10% FBS, 2% penicillin and streptomycin.All cells were cultivated in 5% CO2 at 37℃. To verify whether the predicted hub genes may participate in the formation of ISR, we established two cell models of ISR mechanism with HUVECs and A7r5. HUVECs were stimulated for 24h used 10ng/ml TNF-α as the endothelial (EC) inflammation model. A7r5 was starved for 24h and stimulated for 24h used 20ng/ml PDGF-BB or 20%FBS as the vascular smooth muscle (VSMC) proliferation model.

Assessment of the mRNA expression of hub genes using qRT-PCR

Total RNA was extracted from cells using TRIzol (vazyme, Nanjing, China) according to the manufacturer's instructions. Total RNA was reverse transcribed into cDNA using a cDNA Synthesis Kit (vazyme, Nanjing, China). mRNA levels were tested using QuantStudio Real-Time PCR System Software (Thermo Fisher Scientific, Waltham, MA, USA). The relative expression level for each target gene was normalized by the Ct value of β-actin (internal control) using a $2^{-\Delta\Delta Ct}$ relative quantification method. The relative mRNA expression level of TNF- α and PCNA were used to verify whether the two models were successfully constructed. Triplicate biological replicates were examined for each group and data were representative of multiple independent experiments ($n \geq 3$). A meaningful analysis between the two groups was performed by an unpaired t-test, and a P value < 0.05 was considered statistically significant.

RESULTS

DEG analysis

Here, 12 LIMA samples from 4 CABG patients with stable angina and 3-vessel coronary atherosclerotic lesions from GSE19136 datasets were analyzed. After pre-processing, the raw data were normalized. Based on the cut-off criteria (P value < 0.05 and log2 |foldchange (FC)| > 1), a total of 759 DEGs were identified, including 389 up-regulated (The relative expression was high in PES group and low in BMS group) and 370 down-regulated (The relative expression was low in PES group and high in BMS group) DEGs. A top 100 DEG expression heat map and volcano map were shown in Figure 1a and 1b.

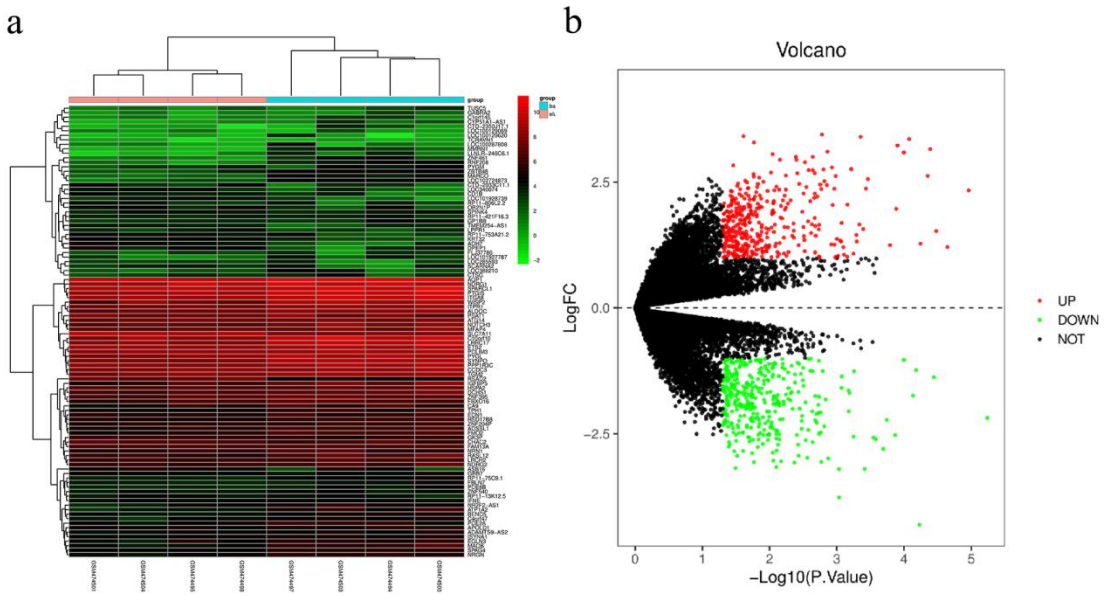

Figure 1. Heatmap and volcano plot of all DEGs between LIMA with different stents. a. Heatmap of DEGs. Each column represents LIMA samples implanted BMS or PES, and each row represents a DEG. The gradual color change from red to green indicates the changing process from upregulation to downregulation. **b.** Volcano plot of DEGs. Green and red dots represent DEGs with log2|foldchange| > 1. *P* value < 0.05. LIMA, left internal mammary artery; BMS, bare metal stent; PES, paclitaxel-eluting stent; DEGs, differentially expressed genes.

Functional enrichment analysis

The significantly different genes were divided into up-regulated and down-regulated groups. The total GO and KEGG analysis were carried out respectively. The results of analysis in R language and metascape were highly correlated, mainly in cell proliferation, migration, up-regulation of chemokines, immune cell activation and inflammatory pathway. At the same time, some studies on in-stent restenosis show that its pathogenic genes and functions mainly focus on inflammation, immune activation, cell cycle, proliferation and migration. In addition, we pay

special attention to some rare metabolic and functional pathways, including NABA matrisome associated, tryptophan metabolism, response to zinc ion pathway and so on. The results of the enrichment analysis were all shown in Figure 2a, 2b, Figure 3a, 3b, Figure 4a-d, Figure 5a and Figure 5b.

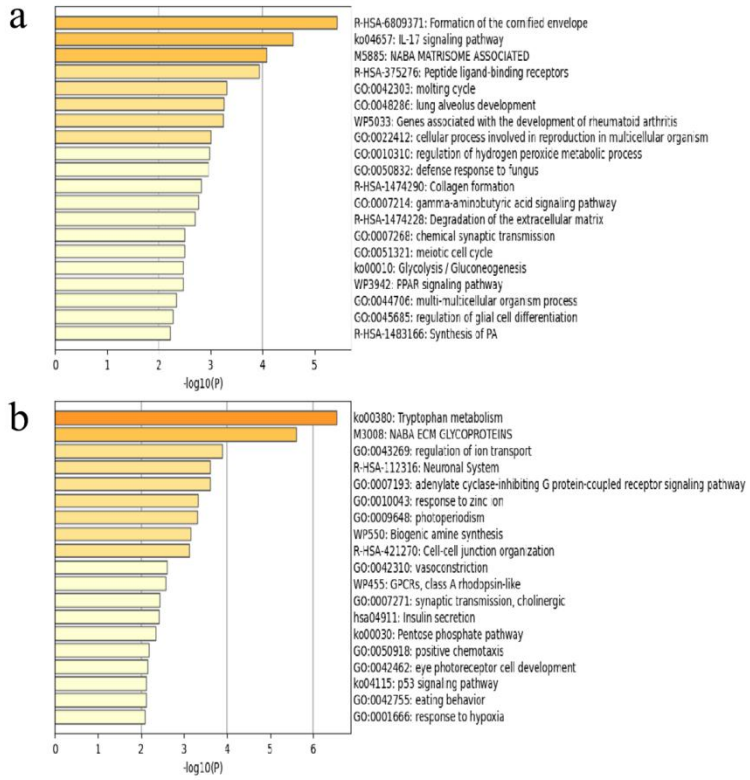

Figure 2. Comprehensive enrichment results of DEGs in up-regulated group and down-regulated group. Using the online enrichment tool Metascape, the DEGs in up-regulated group and down-regulated group are comprehensively enriched and sorted according to the *P* value of the pathway (*P* value < 0.05). **a.** DEGs in the down-regulated group. **b.** DEGs in the up-regulated group. The y-axis labels represent clustered terms; x-axis represent -log10 (*P* value).

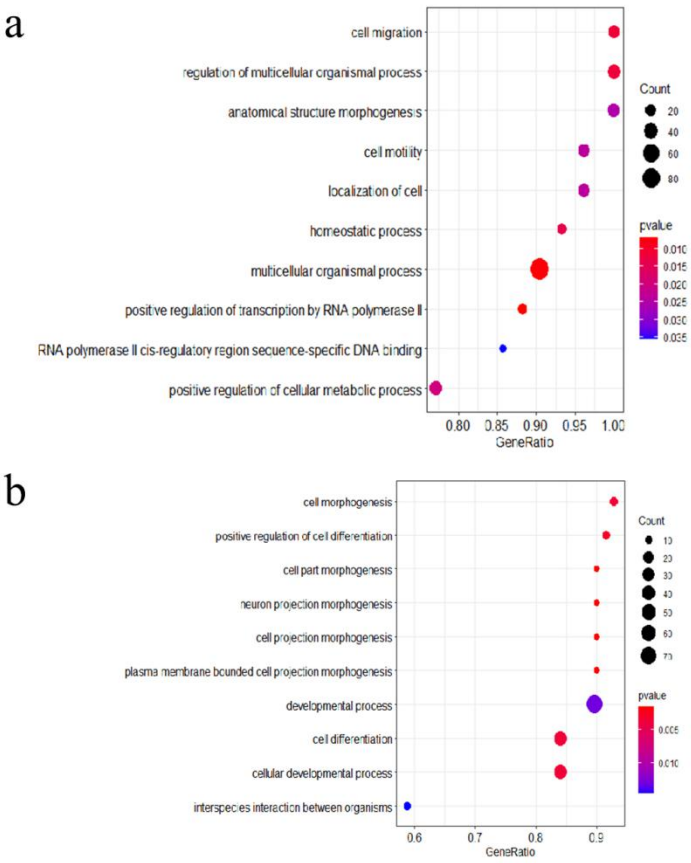

Figure 3. The top 10 significant GO terms enriched in R language. a. DEGs in the down-regulated group. **b.** DEGs in the up-regulated group. GO, gene ontology.

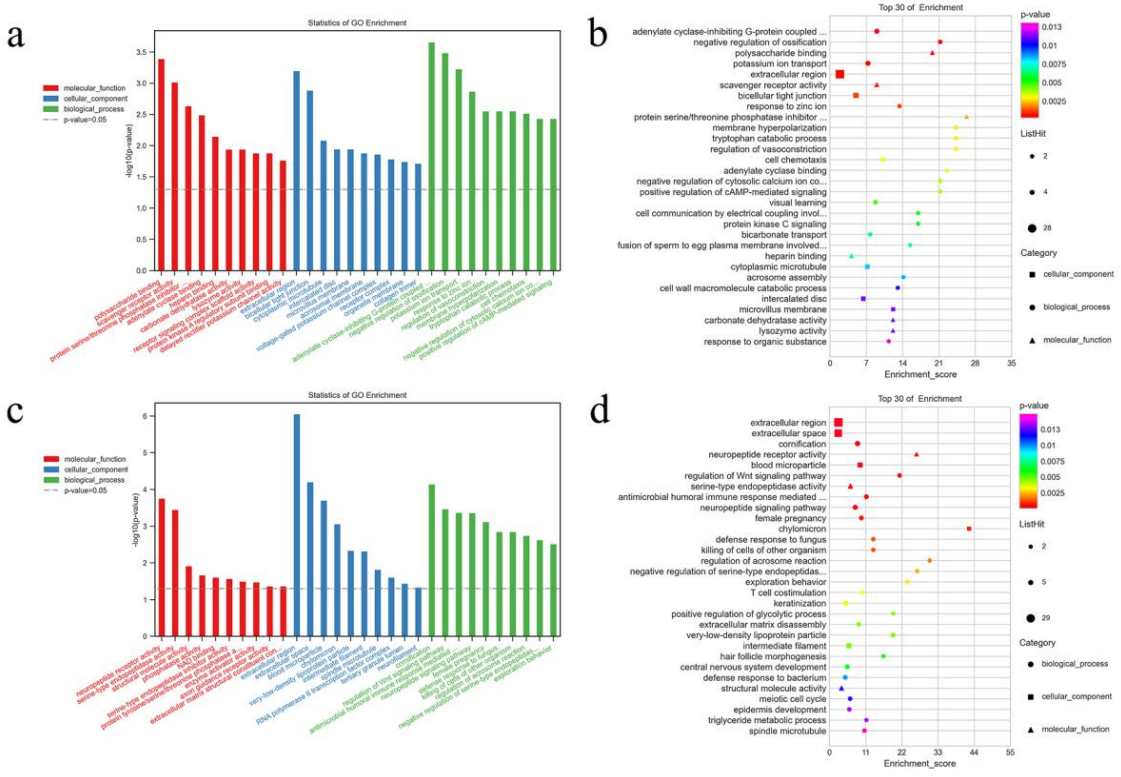

Figure 4. The top 10 significant GO terms in BP, CC, MF. a. The column of DEGs in the up-regulated group. **b.** The bubble plots of DEGs in the up-regulated group. **c.** The column of DEGs in the down-regulated group. **d.** The bubble plots of DEGs in the down-regulated group. BP, biological process; CC, cellular component; MF, molecular function.

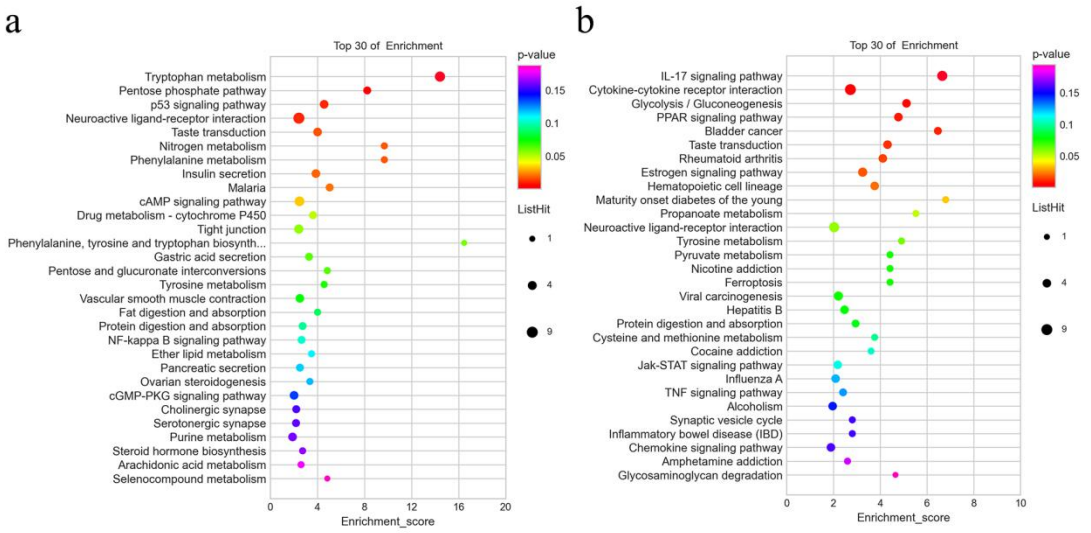

Figure 5. The top 30 KEGG pathways enriched by DEGs in two groups. a. The bubble plots of DEGs in the up-regulated group. **b.** The bubble plots of DEGs in the down-regulated group. KEGG, Kyoto Encyclopedia of Genes and Genomes.

Gene set enrichment analysis

Expression data matrix of all genes was submitted to GSEA to test the metabolic and functional pathways that the gene set may be involved in. The results of GSEA are highly correlated with the enrichment results of GO and KEGG. The GSEA results show high repeatability and accuracy compared to KEGG and go analysis Including cell cycle, cell division, inflammatory response, and regulation of the cardiovascular system. Moreover, the analysis results of KEGG showed that the gene was in cell adhesion molecules (CAMs), cystaine and

methionine metabolism, pentose phosphate pathway, which were shown by several ISR studies. At the same time, some rare functions were shown in the results, such as coat proteins (COPII) vehicle coat, COPII coated vehicle car loading and other functions, which were rarely studied in the cardiovascular system, and possibly become a new direction to study the mechanism of ISR. The representive results of GSEA were listed in Figure 6a-i.

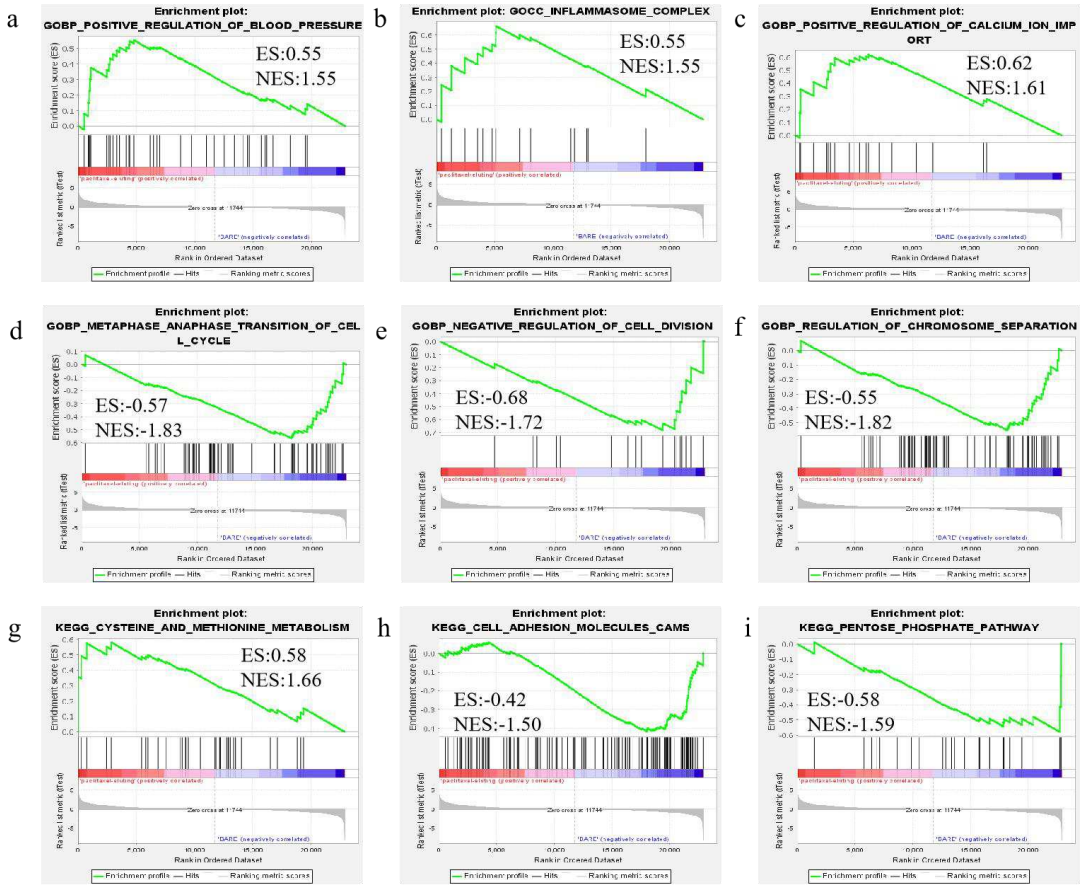

Figure 6. 6 representative GO terms and 3 KEGG pathways from GSEA (*P* value < 0.05). GSEA, gene set enrichment analysis; ES, enrichment score; NES, normalized enrichment score.

a. GOBP: positive regulation of blood pressure. **b.** GOCC: inflammasome complex. **c.** GOBP : positive regulation of calcium ion import. **d.** GOBP metaphase anaphase transition of cell cycle.

e. GOBP negative regulation of cell division. **f.** GOBP regulation of chromosome separation.

g. KEGG cysteine and methionine metabolism. **h.** KEGG cell adhesion molecules cams. **i.** KEGG

pentose phosphate pathway.

PPI network construction and analysis

The 389 up-regulated DEGs and 370 down-regulated DEGs were submitted to the STRING database to predict the interactions between proteins. The PPI network of DEGs was constructed using a combined score greater than 0.4, and the two most significant modules were obtained using MCODE in Cytoscape. Then we selected hub genes from PPI network using the MCC algorithm and cytoHubba plugin. The 9 hub genes of the up-regulated group included ribonucleotide reductase M2 (RRM2), kinesin family member 11 (KIF11), cytoskeleton associated protein 2-like (CKAP2L), GINS complex subunit 2 (GINS2), cell division cycle associated 5 (CDCA5), Rho GTPase activating protein 11A (ARHGAP11A), G-2 and S-phase expressed 1 (GTSE1), minichromosome maintenance complex component 10 (MCM10), centromere protein E (CENPE). The 10 hub gene of the down-regulated group consisted of tachykinin, precursor 1 (TAC1), C – C motif chemokine ligand 4 (CCL4), C-X-C motif chemokine ligand 8 (CXCL8), matrix metallopeptidase 3 (MMP3), leukemia inhibitory factor (LIF), interleukin 5 (IL5), C-C motif chemokine receptor 6 (GPR29/CCR6), interleukin 11 (IL11), matrix metallopeptidase 1 (MMP1), serpin peptidase inhibitor clade B member 2 (SERPINB2). The results were shown in Figure 7a-d.

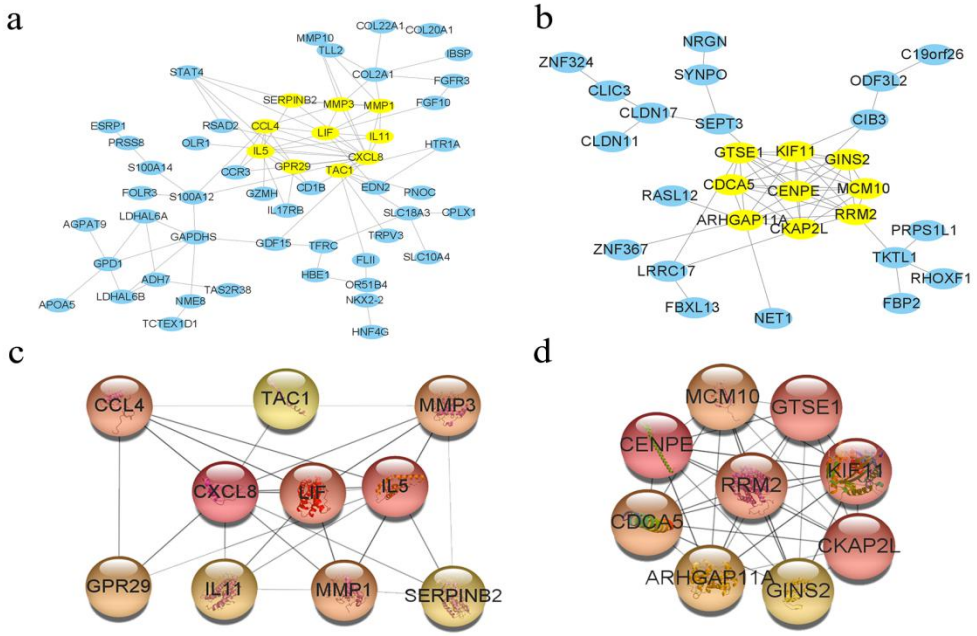

Figure 7. Key modules of PPI networks and hub genes. a. key module of down-regulated DEGs. **b.** key module of up-regulated DEGs. **c.** hub genes of the down-regulated group. **d.** hub genes of the up-regulated group. PPI, protein-protein interaction.

Regulating miRNA prediction

All hub genes selected from Cytoscape were submitted to online tool mirDIP. The top five predicted miRNAs of these genes were selected and presented in Table 1 and Table 2. Among predicted miRNAs, hsa-miR-18a-5p, hsa-miR-122-5p, hsa-miR-24-3p could play significant roles in coronary artery disease (CAD).

Table 1. Predicted miRNA of up-regulated DEGs.

Hub Genes	Predicted miRNAs
RRM2	hsa-miR-93-5p,hsa-let-7i-5p,hsa-miR-519d-3p,hsa-miR-4700-3p, hsa-miR-4666a-3p
KIF11	hsa-miR-381-3p, hsa-miR-122-5p, hsa-miR-4801, hsa-miR-708-3p, hsa-miR-6760-5p
CKAP2L	hsa-miR-5089-5p, hsa-miR-4425, hsa-miR-4781-3p,hsa-miR-4464, hsa-miR-4748
GINS2	hsa-miR-4677-3p, hsa-miR-6726-5p, hsa-miR-668-3P, hsa-miR-4300, hsa-miR-5591-5p
CDCA5	hsa-miR-1296-5p, hsa-miR-221-5p, hsa-miR-1286, hsa-miR-4326, hsa-miR-6763-5p
ARHGAP11A	hsa-miR-4793-5p, hsa-miR-4684-5p, hsa-miR-548ag, hsa-miR-548ai ,hsa-miR-570-5p
GTSE1	hsa-miR-135b-3p, hsa-miR-4467, hsa-miR-8072, hsa-miR-135a-2-3p, hsa-miR-15a-3p
MCM10	hsa-miR-5009-3p, hsa-miR-3153, hsa-miR-194-5p, hsa-miR-4276, hsa-miR-5693
CENPE	hsa-miR-297, hsa-miR-4499, hsa-miR-187-5p, hsa-miR-556-3p, hsa-miR-2053

Table 2. Predicted miRNA of down-regulated DEGs.

Hub Genes	Predicted miRNAs
TAC1	hsa-miR-3675-3p, hsa-miR-1279, hsa-miR-514a-3p, hsa-miR-4797-3p, hsa-miR-4666a-3p
CCL4	hsa-miR-5739, hsa-miR-1843, hsa-miR-24-3p, hsa-miR-765, hsa-miR-4516
CXCL8	hsa-miR-5692a, hsa-miR-573, hsa-miR-4687-3p, hsa-miR-4312, hsa-miR-376a-2-5p
MMP3	hsa-miR-365b-3p, hsa-miR-365a-3p, hsa-miR-623, hsa-miR-146b-3p, hsa-miR-367-5p
LIF	hsa-miR-18a-5p, hsa-miR-18b-5p, hsa-miR-185-5p, hsa-miR-579-3p, hsa-miR-346
IL5	hsa-miR-8084, hsa-miR-4684-5p, hsa-miR-548ag, hsa-miR-548ai, hsa-miR-570-5p
CCR6	hsa-miR-3680-3p, hsa-miR-5581-3p, hsa-miR-4769-3p, hsa-miR-4765, hsa-miR-4774-3p
IL11	hsa-miR-1260a. hsa-miR-1260b, hsa-miR-1224-3p, hsa-miR-5006-3p, hsa-miR-6778-3p
MMP1	hsa-miR-5190, hsa-miR-5094, hsa-miR-514a-5p, hsa-miR-3152-3p, hsa-miR-6857-3p
SERPINB2	hsa-miR-298, hsa-miR-4253, hsa-miR-4649-3p, hsa-miR-4468, hsa-miR-4727-3p

Key TF regulators prediction

All key genes were submitted to the Trrust database for analysis, all possible key TF regulators were obtained, listed in Table 3 and sorted according to their *P* value and FDR (*P* value < 0.05, *FDR* < 0.25), including ETS2, STAT3, NR4A2 and so on, which is highly involved in cardiovascular disease.

Table 3. Predicted key TF regulators of hub genes.

Key TF	Description	Overlapped genes	*P* value	*FDR*
ETS2	v-ets erythroblastosis virus E26 oncogene homolog 2 (avian)	4	1.42e-09	1.84e-08
NFKBIA	nuclear factor of kappa light polypeptide gene enhancer in B-cells inhibitor, alpha	3	1.03e-07	6.72e-07
STAT3	signal transducer and activator of transcription 3 (acute-phase response factor)	4	6.23e-07	2.7e-06
NR4A2	nuclear receptor subfamily 4, group A, member 2	2	2.53e-06	7.82e-06
FOS	FBJ murine osteosarcoma viral oncogene homolog	3	3.09e-06	7.82e-06
CEBPB	CCAAT/enhancer binding protein (C/EBP), beta	3	3.61e-06	7.82e-06
ZFP36	ZFP36 ring finger protein	2	7.07e-06	1.31e-05
ETS1	v-ets erythroblastosis virus E26 oncogene homolog 1 (avian)	3	8.3e-06	1.35e-05
RELA	v-rel reticuloendotheliosis viral oncogene homolog A (avian)	4	1.23e-05	1.65e-05
NFKB1	nuclear factor of kappa light polypeptide gene enhancer in B-cells 1	4	1.27e-05	1.65e-05
JUN	jun proto-oncogene	3	5.56e-05	6.57e-05
GATA3	GATA binding protein 3	2	0.000176	0.000191
EP300	E1A binding protein p300	2	0.000383	0.000383

RT-PCR Validation

RT-PCR was used to detect the expression of hub genes in the up-regulated and down-regulated groups in the total RNA extracted from the cells in the two models. The results of RT-PCR showed that there were significant differences in the expression of CDCA5, LIF, CENPE, KIF11, MMP3, MCM10, ARHGAP11A in the constructed cell model of endothelial inflammation, while there were significant differences in the expression of GTSE1, GINS2, RRM2 and CKAP2L in the model of VSMC proliferation. The examination of two models' buliding were shown in Figure 8a-c and the results of validation in hub genes were shown in Figure 9a-l and Figure 10a-i. (P value < 0.05)

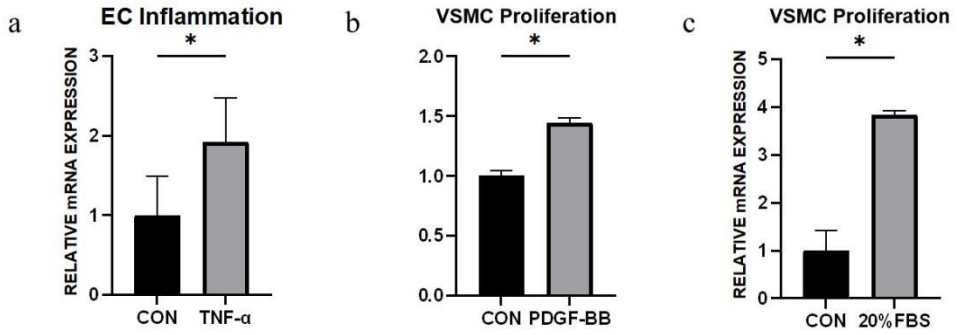

Figure 8. Relative mRNA expression in EC inflammation model or VSMC proliferation model. a. TNF- α relative expression EC inflammation model stimulated for 24h by 10ng/ml TNF- α . **b.** PCNA relative expression VSMC proliferation model stimulated for 24h by 20ng/ml PDGF-BB. **c.** PCNA relative expression in VSMC proliferation model stimulated for 24h by 20%FBS. HUVEC, human umbilical vein endothelial cells; FBS, fetal bovine serum; A7r5, rat thoracic artery smooth muscle cells line.

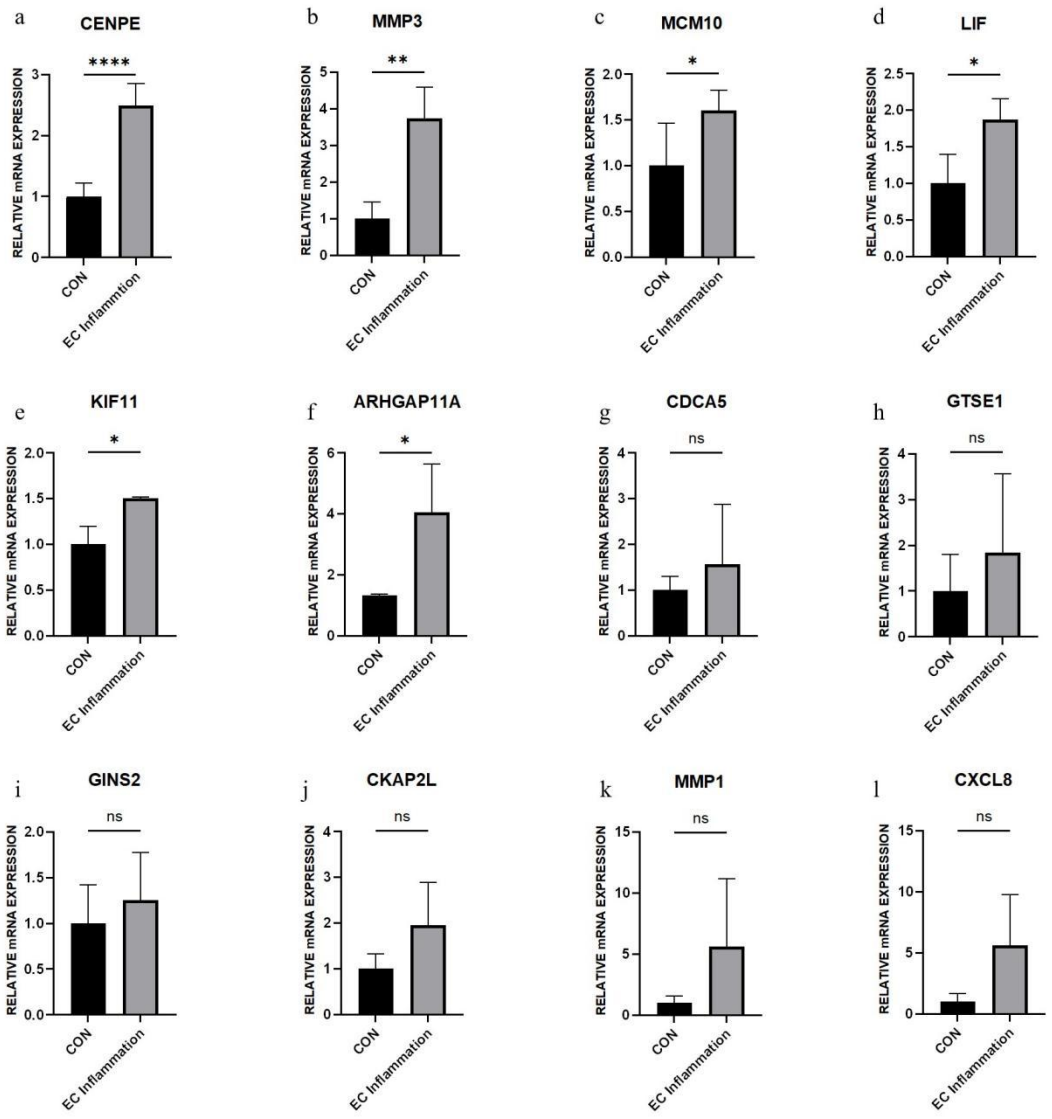

Figure 9. Relative mRNA expression of hub genes in EC inflammation model. a. CENPE. **b.** MMP3. **c.** MCM10. **d.** LIF. **e.** KIF11. **f.** ARHGAP11A. **g.** CDCA5. **h.** GTSE1. **i.** GINS2. **j.** CKAP2L. **k.** MMP1. **l.** CXCL8. ****, *P* value < 0.0001. **, *P* value < 0.01, *, *P* value < 0.05.

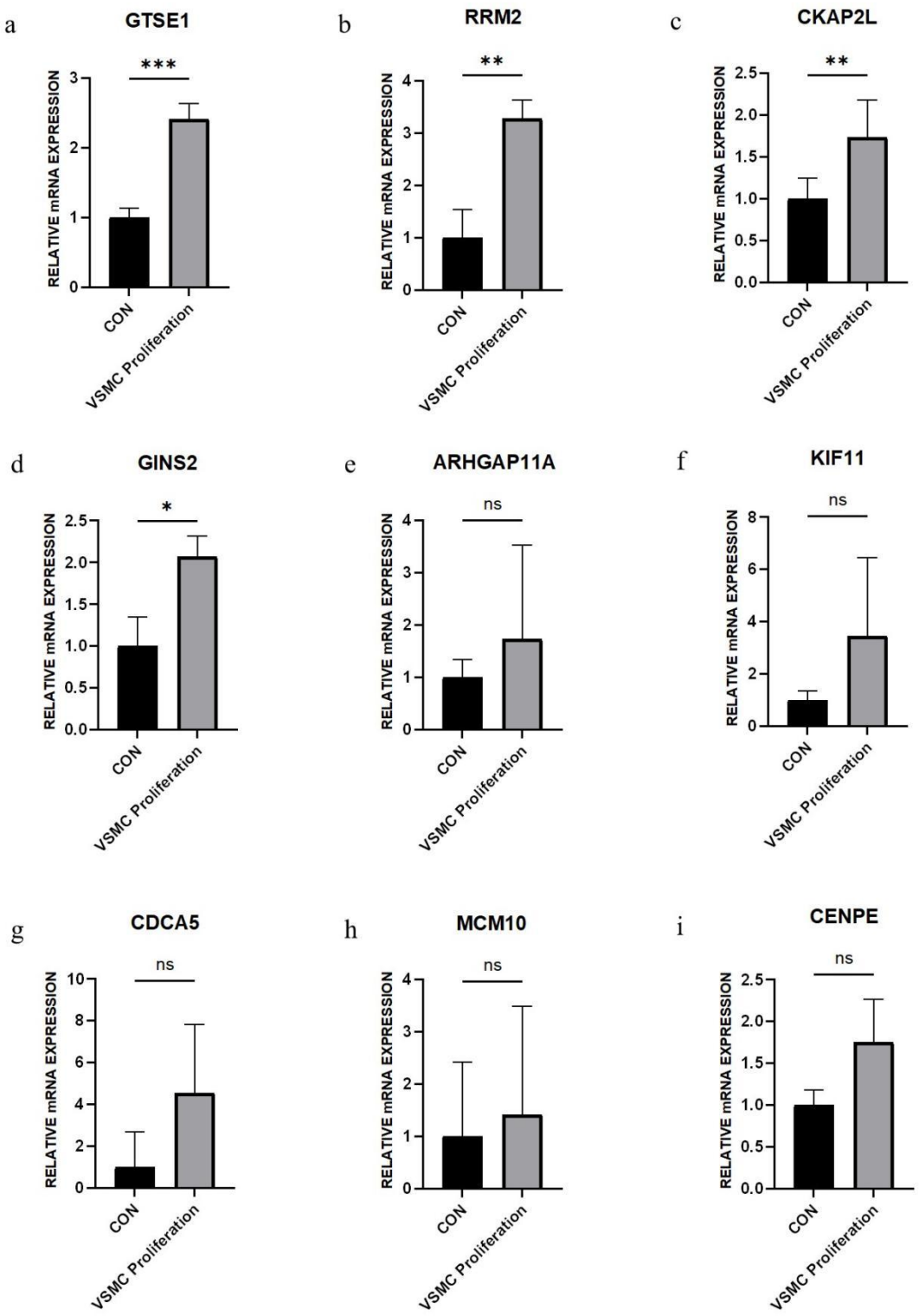

Figure 10. Relative mRNA expression of hub genes in VSMC proliferation model. a. GTSE1. **b.** RRM2. **c.** CKAP2L. **d.** GINS2. **e.** ARHGAP11A. **f.** KIF11. **g.** CDCA5. **h.** MCM10. **i.** CEPNE. ***, *P* value < 0.001. **, *P* value < 0.01, *, *P* value < 0.05.

Discussion

In patients undergoing percutaneous coronary intervention (PCI), the use of DES has greatly reduced the need for reintervention when compared with the use of BMS. Nevertheless, in-stent restenosis continues to remain the principal reason for treatment failure after contemporary coronary stenting[23]. The reason for ISR is unclear, so it is still worth exploring the possible and specific molecular mechanism. The recent development of microarray and bioinformatics has greatly promoted the research on the mechanism of ISR. However, few studies have conducted a comprehensive analysis.

Here, some previous studies have shown the specific mechanism of ISR, including ECs dysfunction, VSMCs proliferation and migration, inflammatory, etc. Studies have shown that endothelial injury, platelet and leukocyte interactions, and subcellular chemoattractant inflammatory mediators are pivotal in the development of the inflammatory response following stent implantation[24]. MMP9 may be involved in the proliferation and migration of endothelial cells associated with atherosclerosis[25]. Meanwhile, when ISR occurred, MMP2 and MMP9 expression decreased in vascular tissue[26], EC dysfunction caused by elevated glucose levels could be useful in exaggerated ISR in diabetes mellitus [27]. In addition, DES inhibits ISR by interfering with the function of VSMCs, like RhoA inhibitor-eluting stent may suppress SMC phenotypic modulation through the inhibition of the YAP signaling pathway [28]. Our results are highly similar to the findings, including some inflammation-related molecules like CXCL8, CCl4, IL-5, etc. CXCL8 is essential for the activation and trafficking of inflammatory mediators[29]. The level of CCL4 is increased in atherosclerotic patients.CCR5 is the receptor of CCL4 and plays an important role in

coronary atherosclerosis[30]. Cooperative induction of CCL4 by TNF-α could lead to metabolic inflammation[31].

Additionally, Go and KEGG enrichment analysis showed that they were enriched in cell cycle, differentiation, migration, metabolism and inflammatory response. Metascape and the R language analysis were highly similar. Most of them are closely related to the mechanism and research progress of ISR. The results of GSEA are highly correlated with the enrichment results of GO and KEGG. Moreover, the analysis results of KEGG showed that the gene was in cell adhesion molecules (CAMs), cystaine and methionine metabolism, pentose phosphate pathway, which were shown by several ISR studies.

Meanwhile, through prediction, we analyzed some new genes and pathways in CAD fields and explained their functions. We found some rare but interesting enrichment functions, such as response to zinc ion, NABA ECM glycoproteins and NABA matrisomeassociated. These functions may require us to pay more attention to their role in ISR. The results of GSEA are highly correlated with the enrichment results of GO and KEGG. At the same time, some rare functions in GSEA were shown in the results, such as COPII vehicle coat, COPII coated vehicle car loading and other functions, which were rarely studied in the cardiovascular system, and possibly become a new direction to study the mechanism of ISR. In all hub genes. We found target genes in RT-PCR validation of the two groups of models, including LIF, CENPE, KIF11, MMP3, MCM10, ARHGAP11A in the EC inflammation model, GTSE1, GINS2, RRM2 and CKAP2L in the VSMC proliferation model. (P value < 0.05)

Some hub genes are highly relevant to CAD. RRM2 encodes one of two non-identical subunits for ribonucleotide reductase and its peptides-conjugated liposome-polycation-DNA

complex (LPD) (RRM2-CLPD) was effectively bound to VSMCs, resulting in significant cellular proliferation and migration inhibition. KIF11 encodes a motor protein[32]. The loss of KIF11 could result in severely stunted growth of the retinal vasculature[33]. CKAP2L is a mitotic spindle protein and its high expression regulated by FOXP3, activates the AKT/mTOR signaling pathway[34], which is also highly related to cardiovascular disease, especially in ISR. CENPE is a kinesin-like motor protein that accumulates in the G2 phase of the cell cycle. Knocking out CENPE inhibited the proliferation and induced the apoptosis of primary pulmonary artery smooth muscle cells (PASMCs) in vivo[35]. MMP3 are part of the matrix metalloproteinases (MMPs) family, well-known inflammatory mediators are a family of zinc-dependent proteolytic enzymes that degrade various components of ECM and non-ECM molecules mediating tissue remodeling in both physiological and pathological processes, which is relevant to the mechanism of ISR. Moreover, vascular cell proliferation and apoptosis can also be regulated by MMP3. LIF activates several signaling pathways, including the JAK/STAT3, PI3K/AKT, ERK1/2 and mTOR signaling pathways, and down-regulates the expression levels of inflammatory cytokines such as IL-1β, IL-6 and TNF-α[36-37]. LIF inhibits angiogenesis and decreases endothelial cell proliferation, migration and extracellular proteolysis[38]. But studies have also confirmed that LIF directly promoted activation of STAT3 and increased blood vessel density in mouse eyes[36].

GINS2, CDCA5, GTSE1, MCM10 and ARHGAP11A have been widely studied in oncology. They are related to the proliferation and apoptosis of many tumor cells and are involved in tumor proliferation, invasion, metastasis and prognosis[39-43]. The research on CAD field is still blank. We can explore whether they are involved in the formation of ISR and related molecular mechanisms in the CAD field.

Finally, several miRNAs and TFs were predicted using online tools. Among these miRNAs, hsa-miR-18a-5p, hsa-miR-122-5p and hsa-miR-24-3p garnered the most attention and predicted TFs regulators are highly related to CAD including EC and VSMC function[44-46]. Most the predicted miRNAs have not been studied in the CAD field, it is worthy of exploring furthermore.

However, several limitations are associated with our study. In the experiment, we verified the roles of the hub genes by simulating the possible mechanism of in-stent restenosis. The probable reasons are as follows : firstly, due to ethical restrictions, we are unable to obtain the coronary artery tissue of patients with ISR or the corresponding control tissue. Secondly, for animal model construction, due to the limitations of experimental conditions, we can not find a suitable animal to complete the model construction of in-stent restenosis. In addition, for the verification of some hub genes, we did not fully get the ideal results. It may be due to the insufficient expression of genes in ECs or VSMCs, and secondly, there may be problems in the prediction itself. Because the database itself lacks the final "outcome", that is, whether ISR occurs or not, there may be prediction deviation. Meanwhile, we found that the predicted molecules could not be effectively amplified by PCR. We did not put these genes into the results, which may be limited by the use of the model or the low expression in the two cells. We need to further explore the difference and function of their expression through experiments.

Here, we used bioinformatics to compare the effects of BMS and PES on the gene level of blood vessels. These results may help us discover the mechanism of ISR formation and provide us with new targets for predicting, diagnosing and treating ISR. Next, we will further study these genes and pathways at the experimental level, deeply clarify their relationship with ISR, and contribute to the treatment of ISR.

Conclusion

Here, using comprehensive bioinformatics analysis and functional enrichment, We found the potential target genes (LIF, CENPE, KIF11, MMP3, MCM10, ARHGAP11A, GTSE1, GINS2, RRM2 and CKAP2L) inherent ISR by comparing LIMA tissues implanted with two different stents in GSE19136. We identified several potential genes, which are worthy of new exploration for the prevention of ISR in the future.

Declarations

Ethics approval and consent to participate

Not applicable

Consent for publication

Not applicable

Availability of data and material

The datasets generated during analysed are available in the GSE 19136 of GEO database. (https://www.ncbi.nlm.nih.gov/geo/query/acc.cgi?acc=GSE19136).

Competing interests

The authors declare that they have no competing interests.

Funding

This work was supported by the National Natural Science Foundation of China.(No.819702170 to Qi-Lin Ma)

Authors' contributions

Chenxi Liu was responsible for thinking framework, data analysis, experimental operation, manuscript writing and modification. Qilin Ma undertook the funding, design and control of the project. Yuanyuan Kuang and Yubo Liu were responsible for review and modification of the paper. Yi Peng revised manuscript pictures and typesetting. Yinzhuang Zhang, Haodong Gao, Xiangyu Yang, Jia Tang and Li Ma put forward some suggestions for the manuscript. All authors read and approved the final manuscript.

Acknowledgements

We appreciated all the participants and staff of GEO database and contributors of GSE 19136, for their invaluable efforts and contribution.

This work was supported by the National Natural Science Foundation of China. (No.819702170 to Qi-Lin Ma)

References:

1. Dangas GD, Claessen BE and Caixeta A, et al. In-Stent Restenosis in the Drug-Eluting Stent Era. *J. Am. Coll. Cardiol.* 2010; 56: 1897-1907. DOI: 10.1016/j.jacc.2010.07.028.
2. Schaer GL and Zhang C. Implementation of miRNAs to Reduce In-Stent Restenosis in the Future. *J. Am. Coll. Cardiol.* 2015; 65: 2328-2330. Editorial; Comment. DOI: 10.1016/j.jacc.2015.04.008.
3. Kim MS and Dean LS. In-Stent Restenosis. *Cardiovasc Ther* 2011; 29: 190-198. DOI: 10.1111/j.1755-5922.2010.00155.x.
4. Gao C, Xu W and Xiao W, et al. Simvastatin decreases stent-induced in-stent restenosis rate via downregulating the expression of PCNA and upregulating that of p27kip1. *J. Interv. Cardiol.* 2013; 26: 384-391. Journal Article. DOI: 10.1111/joic.12049.
5. Pepe M, Napoli G and Carulli E, et al. Autoimmune diseases in patients undergoing percutaneous coronary intervention: A risk factor for in-stent restenosis? *Atherosclerosis* 2021; 333: 24-31. DOI: 10.1016/j.atherosclerosis.2021.08.007.
6. Barone A, Otero-Losada M and Grangeat AM, et al. Ozonetherapy protects from in-stent coronary neointimal proliferation. Role of redoxins. *Int. J. Cardiol.* 2016; 223: 258-261. Journal Article. DOI: 10.1016/j.ijcard.2016.07.177.
7. Joner M, Farb A and Cheng Q, et al. Pioglitazone inhibits in-stent restenosis in atherosclerotic rabbits by targeting transforming growth factor-beta and MCP-1. *Arterioscler Thromb Vasc Biol* 2007; 27: 182-189. Journal Article; Research Support, Non-U.S. Gov't. DOI: 10.1161/01.ATV.0000251021.28725.e8.

8. Bose D, Leineweber K and Konorza T, et al. Release of TNF-alpha during stent implantation into saphenous vein aortocoronary bypass grafts and its relation to plaque extrusion and restenosis. *Am J Physiol Heart Circ Physiol* 2007; 292: H2295-H2299. Clinical Trial; Journal Article; Research Support, Non-U.S. Gov't. DOI: 10.1152/ajpheart.01116.2006.
9. Barilli A, Visigalli R and Sala R, et al. In human endothelial cells rapamycin causes mTORC2 inhibition and impairs cell viability and function. *Cardiovasc. Res.* 2008; 78: 563-571. Journal Article; Research Support, Non-U.S. Gov't. DOI: 10.1093/cvr/cvn024.
10. Ritchie ME, Phipson B and Wu D, et al. limma powers differential expression analyses for RNA-sequencing and microarray studies. *Nucleic Acids Res.* 2015; 43: e47. Journal Article; Research Support, Non-U.S. Gov't. DOI: 10.1093/nar/gkv007.
11. H. Wickham. ggplot2: Elegant Graphics for Data Analysis. Springer-Verlag New York, 2016.,
12. Raivo Kolde (2019). pheatmap: Pretty Heatmaps. R package version 1.0.12. https://CRAN.R-project.org/package=pheatmap,
13. Yu G, Wang LG and Han Y, et al. clusterProfiler: an R package for comparing biological themes among gene clusters. *Omics* 2012; 16: 284-287. Journal Article; Research Support, Non-U.S. Gov't. DOI: 10.1089/omi.2011.0118.
14. Hadley Wickham (2019). stringr: Simple, Consistent Wrappers for Common String Operations. R package version 1.4.0. https://CRAN.R-project.org/package=stringr.
15. Zhou Y, Zhou B and Pache L, et al. Metascape provides a biologist-oriented resource for the analysis of systems-level datasets. *Nat Commun* 2019; 10: 1523. Journal Article; Research Support, N.I.H., Extramural. DOI: 10.1038/s41467-019-09234-6.
16. Szklarczyk D, Gable AL and Lyon D, et al. STRING v11: protein-protein association networks with increased coverage, supporting functional discovery in genome-wide experimental datasets. *Nucleic Acids Res.* 2019; 47: D607-D613. Journal Article; Research Support, N.I.H., Extramural; Research Support, Non-U.S. Gov't; Research Support, U.S. Gov't, Non-P.H.S. DOI: 10.1093/nar/gky1131.
17. Shannon P, Markiel A and Ozier O, et al. Cytoscape: a software environment for integrated models of biomolecular interaction networks. *Genome Res.* 2003; 13: 2498-2504. Journal Article; Research Support, Non-U.S. Gov't; Research Support, U.S. Gov't, Non-P.H.S.; Research Support, U.S. Gov't, P.H.S. DOI: 10.1101/gr.1239303.
18. Bader GD and Hogue CW. An automated method for finding molecular complexes in large protein interaction networks. *Bmc Bioinformatics* 2003; 4: 2. Evaluation Study; Journal Article; Research Support, Non-U.S. Gov't. DOI: 10.1186/1471-2105-4-2.
19. Chin CH, Chen SH and Wu HH, et al. cytoHubba: identifying hub objects and sub-networks from complex interactome. *Bmc Syst Biol* 2014; 8 Suppl 4: S11. Journal Article; Research Support, Non-U.S. Gov't. DOI: 10.1186/1752-0509-8-S4-S11.
20. Subramanian A, Tamayo P and Mootha VK, et al. Gene set enrichment analysis: a knowledge-based approach for interpreting genome-wide expression profiles. *Proc Natl Acad Sci U S A* 2005; 102: 15545-15550. Journal Article. DOI: 10.1073/pnas.0506580102.
21. Tokar T, Pastrello C and Rossos A, et al. mirDIP 4.1-integrative database of human microRNA target predictions. *Nucleic Acids Res.* 2018; 46: D360-D370. Journal Article; Research Support, Non-U.S. Gov't. DOI: 10.1093/nar/gkx1144.
22. Han H, Cho JW and Lee S, et al. TRRUST v2: an expanded reference database of human and

mouse transcriptional regulatory interactions. *Nucleic Acids Res.* 2018; 46: D380-D386. Journal Article; Research Support, Non-U.S. Gov't. DOI: 10.1093/nar/gkx1013.

23. Cassese S, Byrne RA and Schulz S, et al. Prognostic role of restenosis in 10 004 patients undergoing routine control angiography after coronary stenting. *Eur. Heart J.* 2015; 36: 94-99. Journal Article; Multicenter Study. DOI: 10.1093/eurheartj/ehu383.
24. Drachman DE and Simon DI. Inflammation as a mechanism and therapeutic target for in-stent restenosis. *Curr Atheroscler Rep* 2005; 7: 44-49. Journal Article; Review. DOI: 10.1007/s11883-005-0074-5.
25. Zhang G, Yu H and Su J, et al. Identification of Key Genes Associated with Endothelial Cell Dysfunction in Atherosclerosis Using Multiple Bioinformatics Tools. *Biomed Res Int* 2022; 2022: 5544276. Journal Article. DOI: 10.1155/2022/5544276.
26. Shen J, Song JB and Fan J, et al. Distribution and Dynamic Changes in Matrix Metalloproteinase (MMP)-2, MMP-9, and Collagen in an In Stent Restenosis Process. *Eur J Vasc Endovasc Surg* 2021; 61: 648-655. Journal Article; Research Support, Non-U.S. Gov't. DOI: 10.1016/j.ejvs.2020.11.035.
27. Stocca A, O'Toole D and Hynes N, et al. A role for MRP8 in in stent restenosis in diabetes. *Atherosclerosis* 2012; 221: 325-332. Journal Article; Research Support, Non-U.S. Gov't. DOI: 10.1016/j.atherosclerosis.2012.01.036.
28. Huang C, Zhou M and Zheng X. RhoA inhibitor-eluting stent attenuates restenosis by inhibiting YAP signaling. *J. Vasc. Surg.* 2019; 69: 1581-1589. Journal Article; Research Support, Non-U.S. Gov't. DOI: 10.1016/j.jvs.2018.04.073.
29. Ha H, Debnath B and Neamati N. Role of the CXCL8-CXCR1/2 Axis in Cancer and Inflammatory Diseases. *Theranostics* 2017; 7: 1543-1588. Journal Article; Review; Research Support, U.S. Gov't, Non-P.H.S. DOI: 10.7150/thno.15625.
30. Maguire JJ, Jones KL and Kuc RE, et al. The CCR5 chemokine receptor mediates vasoconstriction and stimulates intimal hyperplasia in human vessels in vitro. *Cardiovasc. Res.* 2014; 101: 513-521. Journal Article; Research Support, Non-U.S. Gov't. DOI: 10.1093/cvr/cvt333.
31. Sindhu S, Kochumon S and Shenouda S, et al. The Cooperative Induction of CCL4 in Human Monocytic Cells by TNF-alpha and Palmitate Requires MyD88 and Involves MAPK/NF-kappaB Signaling Pathways. *Int. J. Mol. Sci.* 2019; 20. Journal Article. DOI: 10.3390/ijms20184658.
32. Wu Y, Sun J and Li A, et al. The promoted delivery of RRM2 siRNA to vascular smooth muscle cells through liposome-polycation-DNA complex conjugated with cell penetrating peptides. *Biomed. Pharmacother.* 2018; 103: 982-988. Journal Article. DOI: 10.1016/j.biopha.2018.03.068.
33. Wang Y, Smallwood PM and Williams J, et al. A mouse model for kinesin family member 11 (Kif11)-associated familial exudative vitreoretinopathy. *Hum. Mol. Genet.* 2020; 29: 1121-1131. Journal Article; Research Support, N.I.H., Extramural; Research Support, Non-U.S. Gov't. DOI: 10.1093/hmg/ddaa018.
34. Chi F, Chen L and Jin X, et al. CKAP2L, transcriptionally inhibited by FOXP3, promotes breast carcinogenesis through the AKT/mTOR pathway. *Exp. Cell Res.* 2022; 412: 113035. Journal Article. DOI: 10.1016/j.yexcr.2022.113035.
35. Fang X, Xie M and Liu X, et al. CENPE contributes to pulmonary vascular remodeling in pulmonary hypertension. *Biochem Biophys Res Commun* 2021; 557: 40-47. Journal Article; Research Support, Non-U.S. Gov't. DOI: 10.1016/j.bbrc.2021.04.010.

36. Wang L, Wu Q and Wang RQ, et al. Protection of leukemia inhibitory factor against high-glucose-induced human retinal endothelial cell dysfunction. *Arch. Physiol. Biochem.* 2020: 1-8. Journal Article. DOI: 10.1080/13813455.2020.1792506.
37. Yue X, Wu L and Hu W. The regulation of leukemia inhibitory factor. *Cancer Cell Microenviron* 2015; 2. Journal Article. DOI: 10.14800/ccm.877.
38. Pepper MS, Ferrara N and Orci L, et al. Leukemia inhibitory factor (LIF) inhibits angiogenesis in vitro. *J. Cell Sci.* 1995; 108 (Pt 1): 73-83. Comparative Study; Journal Article; Research Support, Non-U.S. Gov't.
39. Liu X, Sun L and Zhang S, et al. GINS2 facilitates epithelial-to-mesenchymal transition in non-small-cell lung cancer through modulating PI3K/Akt and MEK/ERK signaling. *J. Cell. Physiol.* 2020; 235: 7747-7756. Journal Article; Research Support, Non-U.S. Gov't. DOI: 10.1002/jcp.29381.
40. Xu J, Zhu C and Yu Y, et al. Systematic cancer-testis gene expression analysis identified CDCA5 as a potential therapeutic target in esophageal squamous cell carcinoma. *Ebiomedicine* 2019; 46: 54-65. Journal Article. DOI: 10.1016/j.ebiom.2019.07.030.
41. Lai W, Zhu W and Li X, et al. GTSE1 promotes prostate cancer cell proliferation via the SP1/FOXM1 signaling pathway. *Lab. Invest.* 2021; 101: 554-563. Journal Article; Research Support, Non-U.S. Gov't. DOI: 10.1038/s41374-020-00510-4.
42. Cui F, Hu J and Ning S, et al. Overexpression of MCM10 promotes cell proliferation and predicts poor prognosis in prostate cancer. *Prostate* 2018; 78: 1299-1310. Journal Article. DOI: 10.1002/pros.23703.
43. Xu J, Zhou X and Wang J, et al. RhoGAPs attenuate cell proliferation by direct interaction with p53 tetramerization domain. *Cell Rep* 2013; 3: 1526-1538. Journal Article; Research Support, Non-U.S. Gov't. DOI: 10.1016/j.celrep.2013.04.017.
44. Luo Y, Jiang N and May HI, et al. Cooperative Binding of ETS2 and NFAT Links Erk1/2 and Calcineurin Signaling in the Pathogenesis of Cardiac Hypertrophy. *Circulation* 2021; 144: 34-51. Journal Article; Research Support, N.I.H., Extramural; Research Support, Non-U.S. Gov't. DOI: 10.1161/CIRCULATIONAHA.120.052384.
45. Wang L, Astone M and Alam SK, et al. Suppressing STAT3 activity protects the endothelial barrier from VEGF-mediated vascular permeability. *Dis Model Mech* 2021; 14. Journal Article; Research Support, Non-U.S. Gov't. DOI: 10.1242/dmm.049029.
46. Erl W, Hansson GK and de Martin R, et al. Nuclear factor-kappa B regulates induction of apoptosis and inhibitor of apoptosis protein-1 expression in vascular smooth muscle cells. *Circ. Res.* 1999; 84: 668-677. Journal Article; Research Support, Non-U.S. Gov't. DOI: 10.1161/01.res.84.6.668.